

Analytic structure of meson propagators in the proper-time regularized Nambu–Jona-Lasinio model

Wojciech Broniowski^a, Georges Ripka^b,
Emil N. Nikolov^c, and Klaus Goeke^c

^a *H. Niewodniczański Institute of Nuclear Physics, PL-31342 Cracow, Poland*

^b *Service de Physique Théorique, Centre d'Etudes de Saclay, F-91191 Gif-sur-Yvette Cedex, France*

^c *Institut für Theoretische Physik II, Ruhr-Universität Bochum,
D-44780 Bochum, Germany*



Ruhr-Universität Bochum

Institut für Theoretische Physik II

Teilchen- und Kernphysik

Analytic structure of meson propagators in the proper-time regularized Nambu–Jona-Lasinio model

Wojciech Broniowski^a, Georges Ripka^b,
Emil N. Nikolov^c¹, and Klaus Goeke^c

^a *H. Niewodniczański Institute of Nuclear Physics, PL-31342 Cracow, Poland*

^b *Service de Physique Theorique, Centre d'Etudes de Saclay, F-91191 Gif-sur-Yvette Cedex, France*

^c *Inst. für Theoretische Physik II, Ruhr-Universität Bochum, D-44780 Bochum, Germany*

We analyze the analytic structure of meson propagators in the Nambu–Jona-Lasinio model with a proper-time regulator. We show that the regulator produces unphysical complex singularities. As a result the naive use of the Wick rotation is no longer allowed. Formulas involving integration over mesonic momenta, such as meson-loop contributions or dispersion relations for meson Green's functions, cannot be written in usual forms.

PACS: 12.39.-x, 12.39.Fe, 14.40.Aq

¹ On leave of absence from Institute for Nuclear Research and Nuclear Energy, 1784 Sofia, Bulgaria;
DAAD fellow

² E-mail: wojtek@humboldt.ifj.edu.pl
ripka@amoco.saclay.cea.fr
[emiln or goeke@hadron.tp2.ruhr-uni-bochum.de](mailto:emiln@hadron.tp2.ruhr-uni-bochum.de)

1 Introduction

The purpose of this paper is to discuss analyticity properties of two-point functions in the Nambu–Jona-Lasinio model. We point out that the finite cut-off which regulates the quark loop can lead to unphysical *complex* singularities in mesonic propagators. This is the case of the proper-time regulator. These complex singularities cause complications. For instance, the analytic continuation from the Euclidean to the Minkowski space has to be done with care, since the Wick rotation picks up contributions from these poles (and also, as we will show, from the infinite semi-circle). Other regulators may be free of complex poles (*e.g.* the Pauli-Villars case) but they have other problems.

The presence of complex poles is relevant to calculations of hadronic properties in effective low-energy models (baryon calculations are reviewed *e.g.* in Refs. [1–6], and meson ones in Refs. [7–9]). Properties of baryons found at the soliton, or *mean-field* level, (*e.g.* baryon mass, coupling constants, form factors, *etc.*) are leading- N_c results. These quantities acquire meson-loop corrections, which are $1/N_c$ suppressed. Since $N_c = 3$, some of these formally suppressed effects may be numerically large. When Wick rotations are performed to calculate the meson-loop contributions, the extra complex singularities contribute and may not be neglected.

When discussing the regularization of effective theories, such as the Nambu–Jona-Lasinio model, it is useful to remember that regularization is very different from renormalization, in which a cut-off is introduced and later taken to infinity. The problems discussed in this paper disappear in the limit of infinite cut-off. In the Nambu–Jona-Lasinio model, in order to fit data, we are obliged to work with a finite cut-off which rarely exceeds 1 GeV. QCD does not provide us with a prescription for regularizing the model. Various regularizations have been used. The proper-time regularization of the quark loop is most often used in soliton calculations because it provides us with an action which is a local functional of the fields. This simplifies soliton calculations as well as the definition of conserved currents, which acquire familiar forms. Proper time regularization belongs to the class of regularizations in which only the real part of the Euclidean action is regularized. The reason for not regularizing the imaginary part is two-fold. First, the proper-time regularization can only regularize a positive definite operator, such as DD^\dagger , and it cannot be applied to an operator such as D/D^\dagger , the log of which contributes to the

imaginary part of the Euclidean action². Second, 't Hooft's anomaly matching condition, as well as phenomenology, instruct us that the anomalous processes — those which arise from the imaginary part of the action — should not be regularized.

However, other regularizations exist which yield the correct anomalies: four-momentum regularizations, for example [11–13]. These can be expressed either in terms of momentum-dependent constituent quark masses (or, equivalently, non-local fields) or in terms of cut-off functions which multiply the quark propagators. The non-locality of the resulting model yields extra terms contributing to conserved currents. Four-momentum regularizations can and should be applied to both the real and imaginary parts of the action. They have the attractive feature that anomalous processes turn out to be unregularized. In addition they regularize the theory: both quark and mesons loops are regularized with a single regulator. However, the non-locality induced by the four-momentum cut-off regularizations make the soliton calculations an order of magnitude longer. That is why the proper-time regularization is more often used and why consider it in the present paper.

A further problem with meson loops is the need for introducing a new cut-off. Indeed, the proper-time regularization will regularize the quark loop but not the next-to-leading order meson loop corrections. The regularization of the meson loop introduces an extra parameter in the model to be fixed by some extra physical requirement.

2 The regularized action

We work with the Lagrangian of the $SU(2) \times SU(2)$ -symmetric Nambu–Jona-Lasinio model with scalar and pseudoscalar interactions in the chiral limit of vanishing current quark mass,

$$\mathcal{L} = \bar{\psi} i\partial^\mu \gamma_\mu \psi + \frac{1}{2a^2} \left((\bar{\psi}\psi)^2 + (\bar{\psi}i\gamma_5 \vec{\tau}\psi)^2 \right) . \quad (1)$$

The partition function of the system is given by the path integral

$$\mathcal{Z} \equiv \text{Tr } e^{-\beta H} = \frac{1}{\mathcal{N}} \int \mathcal{D}\phi e^{-S(\phi)} , \quad (2)$$

² The imaginary part of the Euclidean action is odd in the $\epsilon^{\alpha\beta\mu\nu}$ tensor, hence it describes anomalous processes. Conversely, the real part, which does not contain the ϵ tensor, describes non-anomalous processes. See *e.g.* [10].

where ϕ is a four-component chiral field, $\phi = (\phi_0, \phi_1, \phi_2, \phi_3)$, introduced to *partially bosonize* the model [14], and \mathcal{N} is a normalization factor. The Euclidean action $S(\phi)$ consists of a quark part and a mesonic part,

$$S(\phi) = -\text{Tr} \log D + \frac{a^2}{2} \int d^4x \phi^2 , \quad (3)$$

with the Dirac operator and the Dirac Hamiltonian defined as

$$D = \partial_\tau + h , \quad h = -i\vec{\alpha} \cdot \vec{\nabla} + \sum_a \Gamma_a \phi_a . \quad (4)$$

The quark-meson coupling matrices are $\Gamma_0 = \gamma_0$ and $\Gamma_i = i\gamma_0\gamma_5\tau_i$, $i = 1, 2, 3$. The trace in Eq. (3) runs over the quark field variables. The normalization factor in Eq. (2) is equal to $\mathcal{N} = \int \mathcal{D}\phi e^{-\frac{a^2}{2}\phi^2}$.

Most of the discussion of this paper concerns the so-called *proper-time* regularization of the action (3). Indeed it is one of the most widely used regularizations, especially in connection with soliton calculations [15–17]. The proper-time regulated action of the Nambu–Jona-Lasinio model is

$$S_\Lambda(\phi) = \frac{1}{2} \text{Tr} \int \frac{ds}{s} e^{-sD^\dagger D} + \frac{a^2}{2} \int d^4x \phi^2 - \frac{1}{2} \text{Tr} \log(D/D^\dagger) . \quad (5)$$

The first term is the real part of the action, which is regularized, whereas the last term is the imaginary part of the action, which is finite and is not regularized. In our $SU(2)$ -case with no external sources the contribution of the imaginary part vanishes and we drop it.

3 Evaluation of the partition function

We evaluate the partition function (2) using the saddle-point method. The stationary field configuration $\bar{\phi}$ is determined by the equation:

$$\left. \frac{\delta S(\phi)}{\delta \phi_a} \right|_{\phi=\bar{\phi}} = 0 . \quad (6)$$

We consider the case of spontaneously broken chiral symmetry, where all the fields $\bar{\phi}_a$ vanish except one which acquires the non-zero value: $\bar{\phi}_0 = M$. We refer to M as the constituent quark mass. Performing the Gaussian integration over fluctuations of the field

ϕ we get:

$$-\log \mathcal{Z} = S(\bar{\phi}) + \frac{1}{2} \text{Tr} \log(K^{-1}/a^2) , \quad (7)$$

where K^{-1} is the inverse meson propagator, defined as

$$\langle x, a | K^{-1} | y, b \rangle = \frac{\delta^2 S(\phi)}{\delta \phi_a(x) \delta \phi_b(y)} \bigg|_{\phi=\bar{\phi}} . \quad (8)$$

The first term in Eq. (7) is the *quark-loop* contribution and it is proportional to N_c . It is the Hartree term. The second term in Eq. (7) is the *meson-loop* contribution, and it is proportional to N_c^0 . It contains both the Fock term and the RPA correlation energy. The constant a^2 under the log results from the norm \mathcal{N} . Up to now all of the calculations in the soliton sector have been limited to the quark-loop level. In the vacuum sector a few attempts have been made to include the meson-loop effects [18–22].

4 Complex poles of the regularized meson propagators

In this section we analyze the meson propagators K in the vacuum sector when the action is regularized by the proper-time method. We show that the propagator has extra *complex* poles, in addition to the expected singularities corresponding to the on-shell meson pole and the $q\bar{q}$ production threshold. This feature has been overlooked in previous investigations.

Since the chiral symmetry of the vacuum is spontaneously broken, all the fields $\bar{\phi}_a$ vanish except one which acquires the non-zero value: $\bar{\phi}_0 = M$. We refer to M as the constituent quark mass. From (8) we deduce the following inverse pion and σ -meson propagators, which are functions of the Euclidean momentum Q :

$$K_{ab}^{-1}(Q^2) = 4N_c \delta_{ab} (Q^2 + \delta_{a0} 4M^2) f(Q^2) . \quad (9)$$

The function $f(Q^2)$ is equal to:

$$f(Q^2) = \frac{1}{16\pi^2} \int_0^1 du \int_{1/\Lambda^2}^{\infty} \frac{ds}{s} e^{-s(M^2 + Q^2 u(1-u))} = \frac{1}{16\pi^2} \int_0^1 du E_1 \left(\frac{M^2 + Q^2 u(1-u)}{\Lambda^2} \right) \quad (10)$$

with $E_1(z) = \int_1^\infty dt/t e^{-zt}$. Equation (9) implies that the pion propagator ($a = 1, 2, 3$) has a pole at $Q^2 = 0$, and that the σ -meson propagator ($a = 0$) has a pole at $Q^2 = -4M^2$.

These poles are interpreted as on-shell physical particles. On the negative real axis in the Q^2 plane we find, in addition, a quark-antiquark production threshold starting at $Q^2 = -4M^2$, which is an artifact of the lack of confinement. These are well known features of the meson propagators in the Nambu–Jona-Lasinio model.

The meson propagators have, however, additional singularities in the complex Q^2 plane. They are generated by the exponential regulator which appears in the expression (10) of the function $f(Q^2)$. The regulator produces extra *zeros* of the function $f(Q^2)$ in the complex Q^2 plane. This is displayed in Fig. 1, which shows the analytic structure of the pion propagator K^{-1} in the complex Q^2 plane. We see that, in addition to the physical pole and the $q\bar{q}$ cut, there are infinitely many poles which are located close to the imaginary axis. The figure is drawn for the special choice of parameters $\Lambda = M$ (which corresponds to some choice of the parameter a), but the behavior is qualitatively the same for any other choice of parameters. The location of first few poles is: $Q^2/\Lambda^2 = 2.2 \pm 18.0i$, $1.4 \pm 41.7i$, $0.3 \pm 66.6i$, *etc.* ($\Lambda = M$). Asymptotically, for large $|Q^2|$, the real parts of Q^2 at these poles tend to a constant, and imaginary parts are separated by the value $8\pi\Lambda^2$.

The result described above follows from a simple numerical calculation which can be carried out *e.g.* with Mathematica. We just treat Q^2 as a complex variable, and evaluate the integral over the E_1 function in Eq. (10) numerically. The function $E_1(z)$ has a cut from 0 to $-\infty$, and is analytic elsewhere. The integral in Eq. (10) is well behaved, and can be evaluated to any desired accuracy. The appearance of complex zeros of the equation $f(Q^2) = 0$ is not obvious at first glance, and their location cannot be obtained analytically due to the transcendental nature of the function.

A simple example can show why complex zeros appear in functions of this type. Eq. (10) involves averaging over exponential functions. Consider a much simpler case of the function $g(z) = \int_0^1 d\alpha e^{\alpha z} = z^{-1}(e^z - 1)$. This function has zeros at locations $\text{Re}(z) = 0$, $\text{Im}(z) = 2\pi k$ ($k = 0, 1, \dots$), which is very similar to the case shown in Fig. 1. The function of Eq. (10) is clearly more complicated, but the basic structure remains. In Sec. 8 we will encounter another example of this behavior.

The structure such as shown in Fig. 1 is quite peculiar. At first, it might seem that causality and unitarity are violated, since singularities appear off the real negative axis in Q^2 . However, as demonstrated by Lee and Wick [23], and Cutkosky *et al.* [24], there exist models with complex singularities which do satisfy causality and unitarity of the S -matrix.

This is achieved by restricting the in and out scattering states to be composed of stable modes only. Then unitarity of the S -matrix can be maintained. For a two-point function at low values of the s variable, the method of Cutkosky *et al.* is equivalent to calculate Feynman diagrams of the perturbation theory along Wick-rotated contours. At higher values of s pinching of singularities may occur, and the prescription is more involved. Thus, unitarity and (macro)causality [25] may be satisfied, despite the occurrence of complex singularities. An independent study would be required to ascertain whether the prescription may be applied in our case.

Recently Langfeld and Rho [26] analyzed a confining Nambu–Jona-Lasinio-like model in which the pion propagator has, in addition to the physical pole, complex singularities located similarly to our case. In fact, complex singularities appear frequently in model descriptions of confinement (for a review see [27]).

A related problem is the asymptotic behavior of the meson propagator for large values of $|Q|^2$ in the complex plane. In derivations of dispersion relations, or in expressions for the one-meson-loop energy (see Sec. 6), one makes use of the Cauchy theorem. The unregularized meson propagators behave asymptotically as $1/Q^2$, hence the integral over the infinite semi-circle vanishes (after a sufficient number of subtractions), and one obtains the usual dispersion relations. With the finite proper-time cut-off, the asymptotic form of the meson propagator has a form involving an exponential function, $\sim \exp(-\frac{Q^2}{4\Lambda^2})h(Q^2)$, where h is a slowly varying function. In applications of the Cauchy theorem, the contribution from the infinite semi-circle does not vanish. This problem will be discussed in more detail in Sec. 8.

We summarize the problems encountered in the Nambu–Jona-Lasinio model with a proper-time regulator:

- (1) The meson propagators have (infinitely many) extra poles which lie close to the imaginary axis in the complex Q^2 plane. After performing the 3-momentum integration, these poles unwind in cuts in the energy variable.
- (2) When performing a Wick rotation, the complex poles contribute. In addition, we get contributions from the infinite semi-circle. As a result, the usual dispersion relations for meson correlators and other Green's functions acquire extra contributions.
- (3) Note, however, that the pathological poles are quite far away from the origin in the complex Q^2 plane. For the case of Fig. 1 (where $M = \Lambda$) the closest poles are about 18 units of Λ^2 away, while the $q\bar{q}$ production threshold is 4 units of Λ^2 away. Thus

in some numerical calculations the presence of these poles may not be immediately noticeable.

(4) In calculations of Green's functions at large values of incoming momenta squared, a prescription like the one in Ref. [24] has to be used in order to satisfy basic requirements of field theory.

All above problems are due to the finiteness of the cut-off. In the limit $\Lambda \rightarrow \infty$ the poles at complex locations are moved to infinity, and the usual analytic structure is recovered.

5 Spectral representation of meson propagators in background soliton fields

In this and the following sections, we limit the number of quark states contributing to the spectral sum (12) so as to maintain the propagator K finite even in the limit of infinite cut-off. This allows us to obtain a better understanding of the extra poles which are produced by the proper-time regulator.

We extend our results to the general case with arbitrary background fields, *e.g.* for solitons. We make use of the spectral representation, given by the eigenstates of the Dirac Hamiltonian with the meson fields in a saddle-point configuration:

$$h | j \rangle = \left(-i\vec{\alpha} \cdot \vec{\nabla} + \sum_a \Gamma_a \bar{\phi}_a \right) | j \rangle = \epsilon_j | j \rangle, \quad \langle \vec{x} | j \rangle = q_j(\vec{x}) . \quad (11)$$

A straightforward calculation, outlined in App. A, yields the following expression for the inverse meson propagator

$$\begin{aligned} \langle \vec{x}, a | K^{-1}(\nu) | \vec{y}, b \rangle &= \delta(\vec{x} - \vec{y}) \delta_{ab} a^2 + \frac{1}{4\sqrt{\pi}} \sum_{jk} \left(q_j^\dagger(\vec{x}) \Gamma_a q_k(\vec{x}) \right) \left(q_k^\dagger(\vec{y}) \Gamma_b q_j(\vec{y}) \right) \times \\ &\int_{1/\Lambda^2}^{\infty} \frac{ds}{\sqrt{s}} \left(-e^{-s\epsilon_j^2} - e^{-s\epsilon_k^2} + s \left((\epsilon_j + \epsilon_k)^2 + \nu^2 \right) \int_{-1}^1 \frac{du}{2} e^{-\frac{s}{4}(2(\epsilon_k^2 + \epsilon_j^2) + \nu^2 + 2(\epsilon_k^2 - \epsilon_j^2)u - \nu^2 u^2)} \right) . \end{aligned} \quad (12)$$

Note that the sum over the indices j and k runs over *all* the quark states and that it includes a sum over color. In the infinite cut-off case Eq. (12) reduces to the standard expression for the RPA propagator [28–30]:

$$\langle \vec{x}, a \mid K_{\Lambda \rightarrow \infty}^{-1}(\nu) \mid \vec{y}, b \rangle = \delta(\vec{x} - \vec{y}) \delta_{ab} a^2 - \sum_{ph} \left(\frac{\left(q_p^\dagger(\vec{x}) \Gamma_a q_h(\vec{x}) \right) \left(q_h^\dagger(\vec{y}) \Gamma_b q_p(\vec{y}) \right)}{\epsilon_p - \epsilon_h + i\nu} + \frac{\left(q_h^\dagger(\vec{x}) \Gamma_a q_p(\vec{x}) \right) \left(q_p^\dagger(\vec{y}) \Gamma_b q_h(\vec{y}) \right)}{\epsilon_p - \epsilon_h - i\nu} \right), \quad (13)$$

where the labels p and h denote empty particle ($\epsilon_p > 0$) and occupied hole ($\epsilon_h < 0$) states. (A finite quark chemical potential μ_q can be introduced so as to include possible valence states in the set of occupied hole states.) In expression (13) the sum is restricted to particle-hole excitations. This follows “automatically” from Eq. (12). As $\Lambda \rightarrow \infty$, the contributions to the spectral sum from pairs of states with the same sign of the energy vanish identically. This is the expected Pauli-blocking effect.

6 Energy of the soliton at the one-meson-loop level

For the case where the background fields $\bar{\phi}$ are stationary, the expression for the energy of the system is

$$E = -\frac{1}{\beta} \log \mathcal{Z} = E_0 + E_1 - \text{vac} , \quad (14)$$

where E_0 is the contribution obtained in the saddle-point approximation containing the quark loop, and E_1 is the contribution from the one-meson loop. The vacuum energy (vac) is subtracted. The leading saddle-point contribution, which is of order N_c is:

$$E_0 = \frac{1}{4\sqrt{\pi}} \sum_j \int \frac{ds}{s^{3/2}} e^{-s\epsilon_j^2} + \frac{a^2}{2} \int d^3x \sum_a \bar{\phi}_a(\vec{x})^2 . \quad (15)$$

All soliton calculations up to now have been limited to this leading-order contribution. In order to make contact with familiar many-body theory, we define the quark-quark interaction:

$$V_{ij,lk} = - \int d^3x \sum_a \left(q_j^\dagger(\vec{x}) \Gamma_a q_i(\vec{x}) \right) \frac{1}{a^2} \left(q_k^\dagger(\vec{x}) \Gamma_a q_l(\vec{x}) \right) . \quad (16)$$

Making use of Eq. (6) we can cast the quark-loop contribution in the form:

$$E_0 = \frac{1}{4\sqrt{\pi}} \sum_j \int_{\frac{1}{\Lambda^2}}^{\infty} \frac{ds}{s^{3/2}} e^{-s\epsilon_j^2} - \frac{1}{2} \sum_{jk} V_{jj,kk} \frac{1}{4\pi} \int_{\frac{1}{\Lambda^2}}^{\infty} \frac{ds}{s^{1/2}} \epsilon_j e^{-s\epsilon_j^2} \int_{\frac{1}{\Lambda^2}}^{\infty} \frac{ds'}{s'^{1/2}} \epsilon_k e^{-s'\epsilon_k^2} . \quad (17)$$

The second term is recognized as the Hartree energy shown diagrammatically in Fig. 2. In the limit $\Lambda \rightarrow \infty$, the expression (17) reduces to the familiar expression of the Hartree

energy:

$$\lim_{\Lambda \rightarrow \infty} E_0 = \sum_h \epsilon_h - \frac{1}{2} \sum_{hh'} V_{hh,h'h'} , \quad (18)$$

The one-meson-loop contribution is

$$E_1 = \frac{1}{2} \int_{-\infty}^{\infty} \frac{d\nu}{2\pi} \text{Tr} \log \left(K^{-1}(\nu)/a^2 \right) = \frac{1}{2} \int_{-\infty}^{\infty} \frac{d\nu}{2\pi} \log \text{Det} \left(K^{-1}(\nu)/a^2 \right) , \quad (19)$$

with K^{-1} given by Eq. (12). In the infinite cut-off limit we may use the Cauchy theorem to evaluate the integral over ν in Eq. (19). As shown in App. B, the integral of a log of a (well behaved) function f is proportional to the sum over all *zeros* of f in the upper complex plane, minus sum over *poles* of f in the upper complex plane. In our case f equals to $\text{Det}(K_{\Lambda \rightarrow \infty}^{-1}/a^2)$. The zeros correspond to the eigen frequencies ν which satisfy the equation

$$\text{Det} K_{\Lambda \rightarrow \infty}^{-1}(\nu) = 0 , \quad (20)$$

which is the usual RPA equation (see also App. C). The poles of $\text{Det} K_{\Lambda \rightarrow \infty}^{-1}$ are located at the particle-hole excitation energies, as seen from Eq. (13). As a result, we obtain

$$\lim_{\Lambda \rightarrow \infty} E_1 = \frac{1}{2} \int_{-\infty}^{\infty} \frac{d\nu}{2\pi} \log \text{Det} \left(K_{\Lambda \rightarrow \infty}^{-1}(\nu)/a^2 \right) = \frac{1}{2} \sum_{\omega_i > 0} \omega_i - \frac{1}{2} \sum_{ph} (\epsilon_p - \epsilon_h) , \quad (21)$$

where

$$\omega_i = \text{Im}(\nu_i^0) \quad (22)$$

In App. C we show that Eq. (21) may be rewritten as

$$\lim_{\Lambda \rightarrow \infty} E_1 = -\frac{1}{2} \sum_{i>0} \omega_i |Y_i|^2 - \frac{\langle P^2 \rangle}{2M} + \frac{1}{2} \sum_{ph} V_{ph,hp} . \quad (23)$$

We recognize here the usual RPA expression, with a zero-mode contribution [28–30]. The last term is the Fock term, represented diagrammatically in Fig. 3(a). The ring diagrams of Fig. 3(b-c) represent the RPA correlation energy. Note that the meson-loop energy is not just the sum over the RPA frequencies of the form $\frac{1}{2} \sum_i \omega_i$, as sometimes claimed [6,31]. The form of Eq. (23) comes from the $q\bar{q}$ substructure of the meson propagator. Indeed, in purely mesonic models such as the Skyrme model, $E_1 = \frac{1}{2} \sum_i \omega_i$ at the N_c^0 level.

As mentioned before, E_1 is suppressed by one power of N_c compared to E_0 . However, many-body physics provides examples of $1/N_c$ -suppressed results which are important. One effect is the so-called zero-mode correction, which accounts for spurious contributions of the center-of-mass motion. The mean field approximation used in soliton calculations does not separate the center-of-mass coordinates from intrinsic coordinates. This notorious problem of projecting out the center-of-mass motion of solitons has attracted a lot of attention [31–38] and numerical estimates give a negative contribution of the order of 300 MeV. Some estimates [39] use an expression derived for systems with a finite number of particles in the RPA approximation, as in Eq. (23)

$$\Delta M = -\frac{\langle P^2 \rangle}{2M} \quad (24)$$

where P is the momentum operator, and M the soliton mass. In general, such a zero-mode subtraction appears for every continuous symmetry of the Lagrangian which is broken by the solitonic solution. In addition to the translational invariance, hedgehog solitons appearing in chiral models also break the rotational and isospin symmetry, leaving only the sum of spin and isospin preserved. In analogy to Eq. (24) this leads to another subtraction $\Delta M = -\langle J^2 \rangle/(2\Theta)$, where J is the angular momentum operator, and Θ is the moment of inertia [40]. For typical model parameters, the rough estimates of the zero-mode corrections are large, up to 30% of the soliton mass, as expected.

In the derivation of Eq. (23) the Wick rotation has been used. As will be shown in next sections, extra contributions arise when the proper-time regulator is present, and expressions as Eq. (23) do not hold.

7 Finite proper-time cut-off

We decompose the integrals over s as follows:

$$\int_{1/\Lambda^2}^{\infty} ds = \int_0^{\infty} ds - \int_0^{1/\Lambda^2} ds , \quad (25)$$

and use

$$\int_0^{1/\Lambda^2} \frac{ds}{\sqrt{s}} e^{-sr} = \frac{\sqrt{\pi} \operatorname{erf} \left(\frac{\sqrt{r}}{\Lambda} \right)}{\sqrt{r}} , \quad \int_0^{1/\Lambda^2} ds \sqrt{s} e^{-sr} = \frac{\gamma \left(\frac{3}{2}, \frac{r}{\Lambda^2} \right)}{r^{\frac{3}{2}}} = \frac{\sqrt{\pi} \gamma^* \left(\frac{3}{2}, \frac{r}{\Lambda^2} \right)}{2\Lambda^3} , \quad (26)$$

where the error function $\text{erf}(z)$ and the incomplete Euler γ functions $\gamma(n, z)$ and $\gamma^*(n, z)$ are defined *e.g.* in Ref. [41]. We decompose the total contribution to K^{-1} into the infinite cut-off part, and a remainder, which describes the finite-cut-off effects:

$$K^{-1}(\nu) = K_{\Lambda \rightarrow \infty}^{-1}(\nu) + \Delta K^{-1}(\nu) , \quad (27)$$

where

$$\begin{aligned} \langle \vec{x}, a | \Delta K^{-1}(\nu) | \vec{y}, b \rangle &= \frac{1}{4} \sum_{jk} \left(q_j^\dagger(\vec{x}) \Gamma_a q_k(\vec{x}) \right) \left(q_k^\dagger(\vec{y}) \Gamma_b q_j(\vec{y}) \right) \times \\ &\left[- \left(\frac{\text{erf} \left(\frac{|\epsilon_j|}{\Lambda} \right)}{|\epsilon_j|} + \frac{\text{erf} \left(\frac{|\epsilon_k|}{\Lambda} \right)}{|\epsilon_k|} \right) + \right. \\ &\left. \frac{(\epsilon_j + \epsilon_k)^2 + \nu^2}{4\Lambda^3} \int_{-1}^1 du \gamma^* \left(\frac{3}{2}, \frac{\epsilon_k^2 + \epsilon_j^2 + \nu^2/2 + (\epsilon_k^2 - \epsilon_j^2)u - \nu^2 u^2/2}{2\Lambda^2} \right) \right] . \end{aligned} \quad (28)$$

The function $\gamma^*(a, z)$ is an entire function of the variable z (*i.e.* it is single-valued and has no singularities in the finite complex plane – singularities occur only at infinity). Therefore $\langle \vec{x}, a | \Delta K^{-1}(\nu) | \vec{y}, b \rangle$ is also an entire function in the variable ν . This is because ν enters in the argument of γ^* in a non-singular combination with the integration variable u . In other words, $\Delta K^{-1}(\nu)$ has no singularities in the finite complex plane. As a result, the singularities of the function $K^{-1}(\nu)$ are generated by its $\Lambda \rightarrow \infty$ part in Eq. (27). This means they occur at particle-hole excitations, $\nu = \pm i(\epsilon_p - \epsilon_h)$.

The zeros of $\text{Det}K^{-1}(\nu)$ will of course be at different locations than zeros of the $\Lambda \rightarrow \infty$ part. As we change Λ from infinity to a finite value, the zeros of $\text{Det}K^{-1}$ move away from those of $\text{Det}K_{\Lambda \rightarrow \infty}^{-1}$. In addition, new unphysical zeros emerge at complex values of ν . The situation is analogous to the case of the vacuum meson propagators, discussed in Sec. 4.

8 Two-level model

To illustrate how the new zeros of $\text{Det}K$ are generated, we consider a two-level model, in which just one particle state p and one hole state h contribute to the spectral decomposition (12) of the propagator K . In this case only one mesonic fluctuation occurs. Fig. 4 shows the analytic structure of the corresponding inverse meson propagator $K^{-1}(\nu)$ in the complex plane of the energy variable ν . We note the poles (filled dots) located at

$\pm i(\epsilon_p - \epsilon_h)$. The physical zeros (empty dots) on the imaginary axis correspond to the RPA vibration energies. We also see infinitely many unphysical zeros (empty dots) close to the axes at 45° and 135° . If it were drawn in the ν^2 complex plane, Fig. 4 would look very similar to Fig. 1. The displayed structure results from a numerical calculation, where we evaluate expression (12) for the two-level case.

We can carry out an even simpler analysis. Notice that for large values of $|\nu|$, the function K^{-1} in the two-level model can be approximated by:

$$K^{-1}(\nu^2)/a^2 \simeq 1 + b(\nu^2)e^{\frac{-\nu^2}{4\Lambda^2}} , \quad (29)$$

where $b(\nu^2)$ is a slowly varying function. Assuming $b(\nu^2)$ to be a real positive constant, and breaking up ν^2 into real and imaginary parts, $\nu^2 = R + iI$, the zeros of the function K^{-1} occur at the locations

$$I = 4\Lambda^2(2k + 1)\pi , \quad R = -4\Lambda^2 \log b , \quad (30)$$

where k is an integer. The difference between the imaginary parts of successive zeros is $8\pi\Lambda^2$. If we integrate by parts, as in Eq. (B.1), then the integral to be considered is

$$J = \int_{-\infty}^{\infty} d\nu \log(K^{-1}(\nu)/a^2) = - \int_{-\infty}^{\infty} d\nu \nu \frac{dK^{-1}(\nu)/d\nu}{K^{-1}(\nu)} \equiv \int_{-\infty}^{\infty} d\nu j(\nu) . \quad (31)$$

Denoting $\nu = |\nu| e^{i\phi}$, we find that for large $|\nu|$

$$\begin{aligned} j(\nu) &\sim 0 \quad \text{for } \cos(2\phi) > 0 , \\ j(\nu) &\sim \frac{|\nu|^2}{2\Lambda^2} e^{2i\phi} \quad \text{for } \cos(2\phi) < 0 . \end{aligned} \quad (32)$$

This allows us to check if we can close the contour in order to evaluate J via the Cauchy theorem. As a consequence of Eq. (32), the integral of $j(\nu)$ along the contours C_1 and C_3 in Fig. 4 vanishes (this is the case $\cos(2\phi) > 0$), but the integral along the contour C_2 (case $\cos(2\phi) < 0$) *does not vanish*, and is equal to $\sqrt{2} |\nu|^3 / (6\Lambda^2)$. Hence the integral of j over the contour C_2 goes as $|\nu|^3$.

The result is that J in Eq. (31) is an infinite sum of the pole contributions, plus an infinite contribution from the contour C_2 . Since we know that J is finite, cancelations between the infinities from the pole and the C_2 parts occur, and we are left with a finite (but non-zero) result. Certainly, the same cancelation of infinities takes place in the general case of Eq. (19), when we evaluate it via the Cauchy theorem.

9 Other regulators

The analytic structure displayed in Figs. 1 and 4 is specific to the proper-time regulator. Other popular regulators, such as the sharp Euclidean four-momentum cut-off or the Pauli-Villars regulator do not lead to complex singularities. The Pauli-Villars regularization consist of introducing additional families of quarks (which have Bose statistics). In the semi-bosonized form the action has the form

$$\mathcal{L} = -\text{Tr} \log(-i\gamma \cdot \partial + \gamma_0 \Gamma_a \phi_a) + \sum_{p=1}^{N_p} c_p \text{Tr} \log(-i\gamma \cdot \partial + g_p \gamma_0 \Gamma_a \phi_a) + \frac{a^2}{2} \int d^4x \phi^2 , \quad (33)$$

where the the label p labels the Pauli-Villars quark families, N_p is the number of these families, and the constants c_p and g_p are chosen appropriately in order to cancel infinities [42]. It is clear from Eq. (33) that the corresponding meson propagators will have singularities along the real negative Q^2 axis only. Apart from poles, there is the cut going from the $q\bar{q}$ production threshold at $Q^2 = -4M^2$ to $Q^2 = -\infty$, and additional cuts associated with the production of the Pauli-Villars quarks, going from $Q^2 = -4g_p^2 M^2$ to $Q^2 = -\infty$. Therefore the Nambu–Jona-Lasinio model with the Pauli-Villars regulator obeys causality. Moreover, the usual analyticity structure allows for the straightforward use of the Cauchy theorem, rotation of contours, *etc.* In particular, this leads to the formal expression for the RPA correlation energy, such as in Eq. (23). The problem with the Pauli-Villars regulator is that, as remarked in Ref. [43], it violates unitarity. This is because for sufficiently large negative values of Q^2 ($-Q^2 > 4(M^2 + g_p^2 M^2)$) the discontinuity along the cut in meson correlators is negative.

10 Conclusion

We have studied the meson propagators in the Nambu–Jona-Lasinio model in the vacuum and solitonic backgrounds. We have found that the proper-time regularization introduces extra complex poles to the meson propagators, which may cause serious complications. The extra poles, as well as the non-vanishing contribution of the infinite semi-circle, forbid the usual deformation of the energy integration contour which allows one to express the partition function in terms of the physical modes of excitation of the system. The unphysical complex singularities, and the infinite semi-circle piece, have to be accounted for. As a result, the formal connection to well-known text-book expressions is

lost. We no longer have the usual dispersion relations for Green's functions, the RPA-equations for the collective excitations of the system can not be derived in the usual symplectic form. In general, we cannot use the particle-hole description.

In view of this the naive use of the Cauchy theorem in order to calculate the RPA-correlation energy for the Nambu–Jona-Lasinio soliton as *e.g.* in Ref. [31], is incorrect. The correct way to calculate the energy and other observables on the one-meson-loop level is to perform explicitly the integrals over Euclidean four-momenta in the meson propagators.

Our remarks concerning meson correlators also apply to diquark correlators. Diquark models have been formulated in the spirit of the Nambu–Jona-Lasinio model [44–49]. Our warning is that similar care has to be taken while performing integrals over diquark momenta, *e.g.* when continuing diquark functions from the Euclidean to the Minkowski space, or solving the Fadeev equations in quark-diquark systems.

The authors acknowledge the support of the Polish State Committee of Scientific Research, grant 2 P03B 188 09 (WB), the Maria Skłodowska-Curie grant PAA/NSF-95-158, the Bulgarian National Science Foundation, contract Φ-406 (EN), and the Alexander von Humboldt Stiftung (GR, WB), which made this collaboration possible.

A Meson propagators in the spectral representation

We expand the first term in Eq. (5) to second order in mesonic fluctuations $\delta\phi$ around the reference *stationary* state (vacuum, soliton), which has the meson field configuration $\bar{\phi}$. We decompose the $D^\dagger D$ operator as follows: $D^\dagger D = H_0 + V_1 + V_2$, where

$$\begin{aligned} H_0 &= -\partial_\tau^2 + h^2 , \\ V_1 &= -\sum_a (\Gamma_a(\partial_\tau\delta\phi_a) - \{h, \Gamma_a\delta\phi_a\}) , \\ V_2 &= \sum_{ab} \Gamma_a\delta\phi_a\Gamma_b\delta\phi_b . \end{aligned} \quad (\text{A.1})$$

Using the expansion

$$e^{-s(H_0+V)} = e^{-sH_0} - sVe^{-sH_0} + \frac{1}{2}s^2 \int_0^1 d\beta V e^{-s(1-\beta)H_0} Ve^{-s\beta H_0} + \dots \quad (\text{A.2})$$

we pick-up the second-order piece of the proper-time effective action expanded in the mesonic fluctuations $\delta\phi$:

$$S^{F(2)} = \frac{1}{2} \text{Tr}_{1/\Lambda^2} \int ds \left(-V_2 e^{-sH_0} + \frac{1}{2}s \int_0^1 d\beta V_1 e^{-s(1-\beta)H_0} V_1 e^{-s\beta H_0} \right) . \quad (\text{A.3})$$

Now let us use the spectral representation, with states denoted by $|\omega, j\rangle$, etc., where ω is the frequency variable (conjugate to τ) and j is as in Eq. 11. Note that H_0 is diagonal in this representation:

$$H_0 |\omega, j\rangle = (\omega^2 + \epsilon_j^2) |\omega, j\rangle . \quad (\text{A.4})$$

We obtain

$$\langle \vec{x}, a | K^{-1}(\nu) | \vec{y}, b \rangle = \delta(\vec{x} - \vec{y}) \delta_{ab} a^2 + \sum_{jk} (S_{ab}^{jk} + T_{ab}^{jk}) , \quad (\text{A.5})$$

where

$$\begin{aligned} S_{ab}^{jk} &= -\frac{1}{2} (q_j^\dagger(\vec{x}) \Gamma_a q_k(\vec{x})) (q_k^\dagger(\vec{y}) \Gamma_b q_j(\vec{y})) \int \frac{d\omega}{2\pi} \int_{1/\Lambda^2}^\infty ds e^{-s(\omega^2 + \epsilon_j^2)} + (a \leftrightarrow b, \vec{x} \leftrightarrow \vec{y}) , \\ T_{ab}^{jk} &= \frac{1}{4} (q_j^\dagger(\vec{x}) \Gamma_a q_k(\vec{x})) (q_k^\dagger(\vec{y}) \Gamma_b q_j(\vec{y})) \int \frac{d\omega}{2\pi} ((\epsilon_j + \epsilon_k)^2 + \nu^2) \\ &\times \int_{1/\Lambda^2}^\infty ds s \int_0^1 d\beta e^{-s(1-\beta)((\omega-\nu)^2 + \epsilon_k^2)} e^{-s\beta(\omega^2 + \epsilon_j^2)} + (a \leftrightarrow b, \vec{x} \leftrightarrow \vec{y}) . \end{aligned} \quad (\text{A.6})$$

Carrying out the ω integration, changing the integration variable β to $u = 2\beta - 1$, and noticing that the replacement $(a \leftrightarrow b, \vec{x} \leftrightarrow \vec{y})$ is equivalent to $(j \leftrightarrow k, u \leftrightarrow -u)$, we get Eq. (12).

B Integral of the logarithm of a function.

We recall a useful form of an integral of the logarithm of a function f . First, integrate by parts:

$$I = \frac{1}{2} \int_{-\infty}^{\infty} \frac{d\nu}{2\pi} \log f(\nu) = \frac{1}{4\pi} \nu \log f(\nu) \Big|_{-\infty}^{\infty} - \int_{-\infty}^{\infty} \frac{d\nu}{4\pi} \nu \frac{df(\nu)/d\nu}{f(\nu)} . \quad (\text{B.1})$$

Assume that the function f has poles at $\nu = \nu_i^{\text{pole}}$ and zeros at $\nu = \nu_j^0$. Then the function $\nu \frac{df(\nu)/d\nu}{f(\nu)}$ has a set of poles at $\nu = \nu_i^{\text{pole}}$ with residues $-\nu_i^{\text{pole}}$, and another set of poles at $\nu = \nu_j^0$ with residues $+\nu_j^0$. If the surface term vanishes, and if the integral along the infinite upper (or lower) semi-circle vanishes, then the Cauchy theorem gives the following result:

$$I = -\frac{i}{2} \left(\sum_{j>0} \nu_j^0 - \sum_{i>0} \nu_i^{\text{pole}} \right) , \quad (\text{B.2})$$

where $j > 0$ indicates that $\mathcal{Im}(\nu_j^0) > 0$, and $i > 0$ indicates that $\mathcal{Im}(\nu_i^{\text{pole}}) > 0$.

C RPA equations.

It is convenient to use an *orthonormal* basis in the mesonic space, defined by a set of functions $f_n(\vec{x})$. Each f_n is a four-component vector in the σ , π_1 , π_2 , and π_3 space, *i.e.* $f_n = (f_n^0, f_n^1, f_n^2, f_n^3)$. We define

$$K_{mn}^{-1}(\nu) = \sum_{ab} \int d^3x \int d^3y f_m^a(\vec{x}) \langle \vec{x}, a \mid K^{-1}(\nu) \mid \vec{y}, b \rangle f_n^{b*}(\vec{y}) . \quad (\text{C.1})$$

Condition (20) is equivalent to solving the eigenvalue problem (everywhere below repeated indices are summed over)

$$\lim_{\Lambda \rightarrow \infty} K_{mn}^{-1}(\nu) f_n = 0 . \quad (\text{C.2})$$

Defining the quark-meson overlap coefficients as

$$C_m^{jk} = \sum_a \int d^3x q_j^\dagger(\vec{x}) \Gamma_a q_k(\vec{x}) f_m^a(\vec{x}) \quad (C.3)$$

we can show that the problem (C.2) is equivalent to the following set of equations:

$$\begin{aligned} C_n^{ph} X^{ph} + C_n^{hp} Y^{hp} + a^2 f_n &= 0 , \\ (\epsilon_p - \epsilon_h + i\nu) X^{ph} + (C_n^{ph})^* f_n &= 0 , \\ (\epsilon_p - \epsilon_h - i\nu) Y^{hp} + (C_n^{hp})^* f_n &= 0 , \end{aligned} \quad (C.4)$$

which can be seen immediately when one eliminates the variables X_n^{ph} and Y_n^{hp} from the above equation — as a result, the original Eq. (C.2) is obtained. One can also eliminate the variables f_n from Eqs. (C.4), using the first of Eqs. (C.4): $f_n = -1/a^2 (C_n^{ph} X^{ph} + C_n^{hp} Y^{hp})$. The second and third equations become:

$$\begin{aligned} (\epsilon_p - \epsilon_h + i\nu) X^{ph} - \frac{1}{a^2} \left((C_n^{ph})^* C_n^{p'h'} X^{p'h'} + (C_n^{ph})^* C_n^{h'p'} Y^{h'p'} \right) &= 0 , \\ (\epsilon_p - \epsilon_h - i\nu) Y^{hp} - \frac{1}{a^2} \left((C_n^{hp})^* C_n^{p'h'} X^{p'h'} + (C_n^{hp})^* C_n^{h'p'} Y^{h'p'} \right) &= 0 . \end{aligned} \quad (C.5)$$

Since the basis $\{f_n\}$ is complete (this is an arbitrary orthonormal basis, e.g. of plane waves), *i.e.* $\sum_n f_n^a(\vec{x}) f_n^{b*}(\vec{y}) = \delta^{ab} \delta(\vec{x} - \vec{y})$, we have

$$-\frac{1}{a^2} \sum_n (C_n^{ij})^* C_n^{kl} = V_{ij,lk} , \quad (C.6)$$

where V has been defined in Eq. (16). Using this notation we may rewrite Eq. (C.5) as

$$\begin{aligned} & \begin{pmatrix} (\epsilon_p - \epsilon_h) \delta_{ph,p'h'} + V_{ph,h'p'} & V_{ph,p'h'} \\ V_{hp,h'p'} & (\epsilon_p - \epsilon_h) \delta_{ph,h'p'} + V_{hp,p'h'} \end{pmatrix} \begin{pmatrix} X^{p'h'} \\ Y^{h'p'} \end{pmatrix} \\ &= -i\nu \begin{pmatrix} \delta_{ph,p'h'} & 0 \\ 0 & -\delta_{ph,h'p'} \end{pmatrix} \begin{pmatrix} X_n^{p'h'} \\ Y_n^{h'p'} \end{pmatrix} \end{aligned} \quad (C.7)$$

This is the symplectic RPA eigenvalue problem, familiar from nuclear physics, which has the form

$$\begin{pmatrix} A & B \\ B^* & A^* \end{pmatrix} \begin{pmatrix} X \\ Y \end{pmatrix} = -i\nu \begin{pmatrix} 1 & 0 \\ 0 & -1 \end{pmatrix} \begin{pmatrix} X \\ Y \end{pmatrix} \quad (\text{C.8})$$

We refer the reader to Refs. [28–30] for a detailed discussion of this symplectic eigenvalue problem. We now want to rewrite the quantity $\sum_{ph}(\epsilon_p - \epsilon_h)$ differently. From Eq. (C.7-C.8) we see that

$$\sum_{ph}(\epsilon_p - \epsilon_h) = \text{Tr}A - \sum_{ph}V_{ph,hp} \quad (\text{C.9})$$

The trace in this expression may be evaluated using the eigenstates of Eq. (C.8), and we get

$$\frac{1}{2}\text{Tr}A = + \sum_{i>0} \omega_i (|X_i|^2 + |Y_i|^2) + \frac{\langle P^2 \rangle}{2M} \quad (\text{C.10})$$

We stress that the above result is *algebraic* in origin, and holds for any symplectic problem. The zero-mode piece $\frac{\langle P^2 \rangle}{2M}$ is generated “automatically”. In hedgehog models there is also an angular-momentum zero-mode piece.

Collecting expressions (21,C.9,C.10) and using the fact that $|X_i|^2 - |Y_i|^2 = 1$ [28–30], we get finally

$$\lim_{\Lambda \rightarrow \infty} E_1 = -\frac{1}{2} \sum_{i>0} \omega_i |Y_i|^2 - \frac{\langle P^2 \rangle}{2M} + \frac{1}{2} \sum_{ph} V_{ph,hp} \quad (\text{C.11})$$

References

- [1] L. Wilets, Nucl. Phys. **A446** (1985) 425c
- [2] I. Zahed and G. E. Brown, Phys. Rep. **142** (1986) 1
- [3] M. K. Banerjee, W. Broniowski, and T. D. Cohen, in *Chiral Solitons*, edited by K.-F. Liu (World Scientific, Singapore, 1987)
- [4] M. C. Birse, Prog. Part. Nucl. Phys. **25** (1990) 1
- [5] T. Meissner, E. Ruiz Arriola, A. Blotz, and K. Goeke, Ruhr-Univ. Bochum preprint No. RUB-TPII-42-93 (1993)
- [6] R. Alkofer, H. Reinhardt, and H. Weigel, Tuebingen U. preprint No. UNITU-THEP-25-1994, hep-ph/9501213 (1994)
- [7] W. Weise, U. Regensburg preprint No. TPR-93-2 (1993)
- [8] U. Vogl and W. Weise, Progr. Part. Nucl. Phys. **7** (1991) 195
- [9] J. Bijnens, Nordita preprint No. 95-10-N-P, hep-ph/9502335 (1995)
- [10] J. A. Zuk, Z. Phys. **C 29** (1985) 303
- [11] C. D. Roberts, R. T. Cahill, and J. Praschifka, Ann. of Phys. (NY) **188** (1988) 20
- [12] B. Holdom, J. Terning, and K. Verbeek, Phys. Lett. **B 232** (1989) 351
- [13] R. D. Ball and G. Ripka, in *Many Body Physics (Coimbra)*, edited by C. F. et al. (World Scientific, Singapore, 1993)
- [14] T. Eguchi, Phys. Rev. D **14** (1975) 2755
- [15] D. I. Dyakonov and V. Y. Petrov, JETP Lett. **43** (1986) 57
- [16] Th. Meissner, F. Grümmer, and K. Goeke, Ann. Phys. **202** (1990) 297
- [17] H. Reinhardt and R. Wünsch, Phys. Lett. **B 215** (1988) 577

[18] N.-W. Cao, C. M. Shakin, and W.-D. Sun, Phys. Rev. **C46** (1992) 2535

[19] E. Quack and S. P. Klevansky, Phys. Rev. **C49** (1994) 3283

[20] P. Zhuang, J. Hüfner, S. P. Klevansky, and H. Voss, Ann. of Phys. (NY) **234** (1994) 225

[21] V. Dmitrašinović, H.-J. Schulze, R. Tegen, and R. H. Lemmer, Ann. of Phys. (NY) **238** (1995) 332

[22] E. N. Nikolov *et al.*, Univ. of Bochum preprint No. RUB-TPII-13/95 (1995), hep-ph 9602274

[23] T. D. Lee and G. C. Wick, Nucl. Phys. **B 9** (1969) 209

[24] R. E. Cutkosky, P. V. Landshoff, D. I. Olive, and J. C. Polkinghorne, Nucl. Phys. **B 12** (1969) 281

[25] D. Iagolnitzer, *Scattering in Quantum Field Theories* (Princeton University Press, Princeton, New Jersey, 1992)

[26] K. Langfeld and M. Rho, Saclay preprint No. T95/070, hep-ph/9506265 (1995)

[27] C. D. Roberts and A. G. Williams, Prog. Part. Nucl. Phys. **33** (1994) 477

[28] D. J. Rowe, *Nuclear Collective Motion* (Methuen, London, 1970)

[29] P. Ring and P. Schuck, *The Nuclear Many-Body Problem* (Springer, Berlin, 1980)

[30] J.-P. Blaizot and G. Ripka, *Quantum Thory of Finite Systems* (The MIT Press, Cambridge, Massachusetts, 1986)

[31] H. Weigel, R. Alkofer, and H. Reinhardt, Nucl. Phys. **A582** (1995) 484

[32] I. Zahed, A. Wirzba, and U.-G. Meissner, Phys. Rev. D **33** (1986) 830

[33] A. Dobado and J. Terron, Phys. Lett. **B247** (1990) 581

[34] B. Moussalam and D. Kalafatis, Phys. Lett. **B272** (1991) 196

[35] G. Holzwarth, Phys. Lett. **B291** (1992) 218

- [36] G. Holzwarth, Nucl. Phys. **A572** (1994) 69
- [37] E. G. Lubeck, M. C. Birse, E. M. Henley, and L. Wilets, Phys. Rev. D **33** (1986) 234
- [38] B. Golli and M. Rosina, Phys. Lett. **165B** (1985) 347
- [39] P. V. Pobylitsa *et al.*, J. Phys. G **18** (1992) 1455
- [40] W. Broniowski and T. D. Cohen, Phys. Lett. **177B** (1986) 141
- [41] M. Abramowitz and I. A. Stegun (ed.), *Handbook of mathematical functions* (Dover Publications, New York, 1965)
- [42] F. Döring, A. Blotz, C. Schüren, Th. Meissner, E. Ruiz-Arriola and K. Goeke, Nucl. Phys. **A536** (1992) 548
- [43] R. M. Davidson and E. R. Arriola, Phys. Lett. **B 359** (1995) 273
- [44] V. Thorsson and I. Zahed, Phys. Rev. **D41** (1990) 3442
- [45] U. Vogl, Z. Phys. **A337** (1990) 191
- [46] U. Vogl and W. Weise, Prog. Part. Nucl. Phys. **27** (1991) 195
- [47] H. Reinhardt, Phys. Lett. **B244** (1990) 316
- [48] C. Weiss, A. Buck, R. Alkofer, and H. Reinhardt, Phys.Lett. **B312** (1993) 6
- [49] G. Hellstern and C. Weiss, Phys. Lett. **B351** (1995) 64

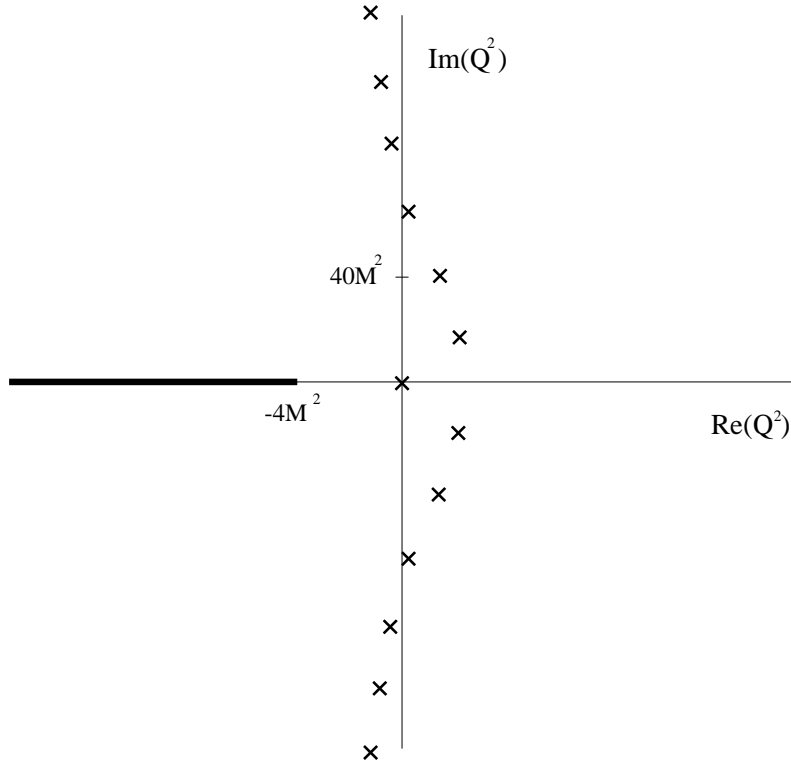


Fig. 1. The analytic structure of the pion propagator in the complex Euclidean momentum plane, Q^2 . It has the physical pole at $Q^2 = 0$, the $q\bar{q}$ production cut from $Q^2 = -4M^2$ to $-\infty$, and unphysical poles located close to the imaginary axis. The parameters are $M = \Lambda$. Note different scales on the real and imaginary axis. The corresponding plot for the σ -meson propagator differs only by the location of the physical pole, which is moved from $Q^2 = 0$ to $Q^2 = -4M^2$.

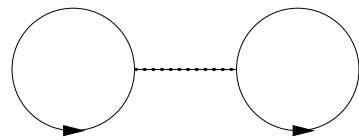


Fig. 2. The Hartree diagram. The dotted line is the interaction, which is local in our case, and carries a factor of $1/N_c$. The diagram is of order N_c .

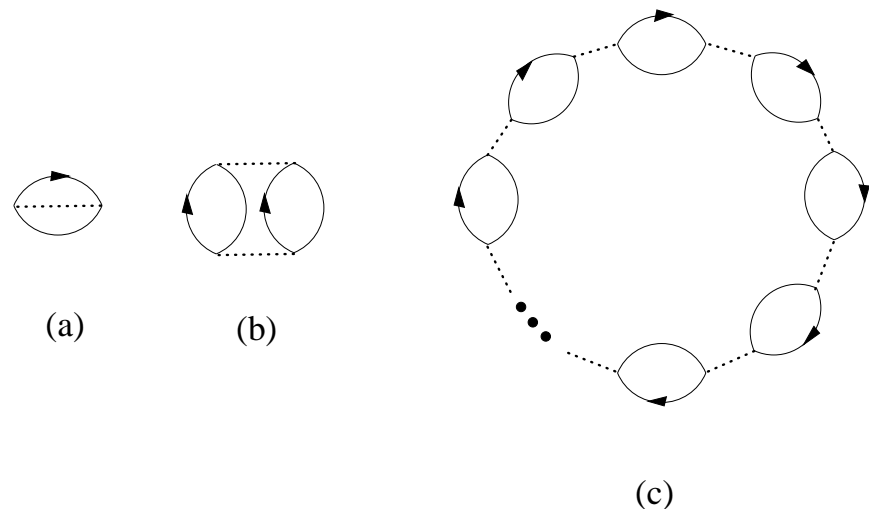


Fig. 3. The Fock diagram (a), and higher order ring diagrams (b-c). All these diagrams are of order N_c^0 .

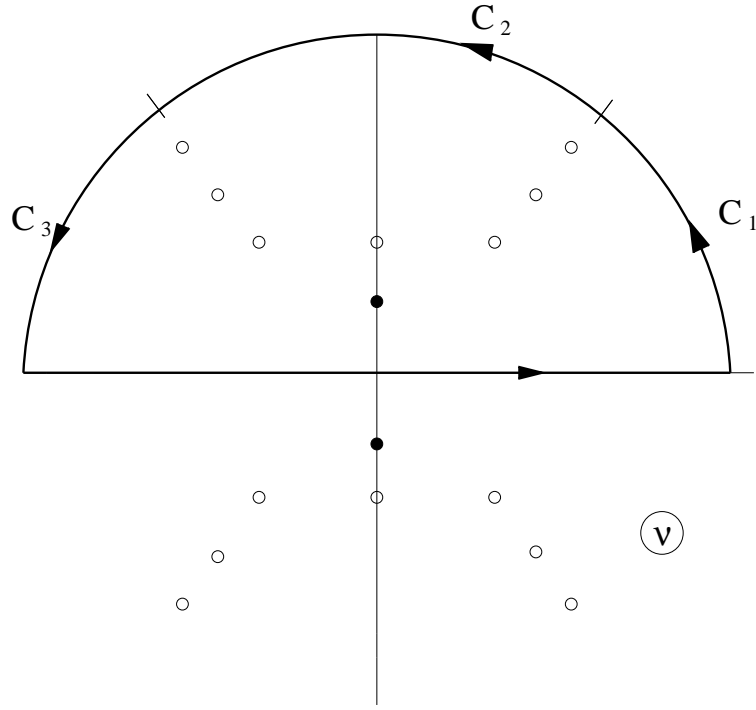
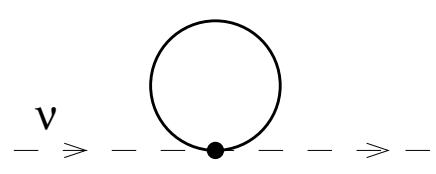
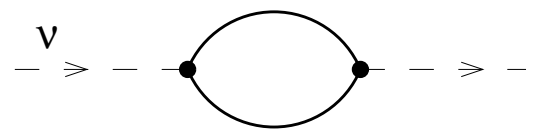


Fig. 4. The analytic structure of the function $K^{-1}(\nu)$. It has poles on the imaginary axis (filled dots), corresponding to particle-hole excitations, and zeros on the imaginary axis (empty dots), corresponding to the RPA vibrations. Additionally, it has infinitely many unphysical zeros in the complex plane off the imaginary axis (empty dots). These zeros become poles of the meson propagator K . The contour integral along C_3 diverges as the radius of the semi-circle goes to infinity. The sum of pole contributions and the C_3 -contribution is finite.



(a)



(b)